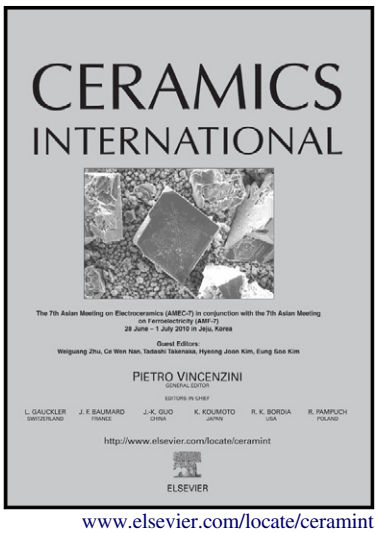

www.elsevier.com/locate/ceramint

Construction of magnetically separable Ag_3PO_4/Fe_3O_4/GO composites as recyclable photocatalysts

Zhenyuan Ji, Junling Zhao, Xiaoping Shen, Xiaoyang Yue, Aihua Yuan, Hu Zhou, Juan Yang

PII: S0272-8842(15)01434-0
DOI: http://dx.doi.org/10.1016/j.ceramint.2015.07.144
Reference: CERI11028

To appear in: *Ceramics International*

Received date: 25 June 2015
Revised date: 22 July 2015
Accepted date: 23 July 2015

Cite this article as: Zhenyuan Ji, Junling Zhao, Xiaoping Shen, Xiaoyang Yue, Aihua Yuan, Hu Zhou, Juan Yang, Construction of magnetically separable Ag_3PO_4/Fe_3O_4/GO composites as recyclable photocatalysts, *Ceramics International,* http://dx.doi.org/10.1016/j.ceramint.2015.07.144

Construction of magnetically separable $Ag_3PO_4/Fe_3O_4/GO$ composites as recyclable photocatalysts

Zhenyuan Ji [a], Junling Zhao [a], Xiaoping Shen [a,*], Xiaoyang Yue [a], Aihua Yuan [b], Hu Zhou [a], Juan Yang [a]

[a] *School of Chemistry and Chemical Engineering, School of Materials Science and Engineering, Jiangsu University, Zhenjiang 212013, P. R. China*

[b] *School of Environmental and Chemical Engineering, Jiangsu University of Science and Technology, Zhenjiang 212003, P. R. China*

* Corresponding author. Tel/Fax: +86-511-88791800

E-mail address: xiaopingshen@163.com (Xiaoping Shen)

Abstract: In this study, a less finicky and effective method is developed to synthesize Ag_3PO_4/Fe_3O_4/graphene oxide (GO) ternary composites. The as-synthesized samples are characterized by X-ray diffraction (XRD), scanning electron microscopy (SEM), and transmission electron microscopy (TEM). The photocatalytic activity of $Ag_3PO_4/Fe_3O_4/GO$ composites is evaluated by degrading Rhodamine B (RhB) under simulated sunlight irradiation. In comparison with bare Ag_3PO_4, the $Ag_3PO_4/Fe_3O_4/GO$ composites show enhanced photocatalytic activity, which can be attributed to the improved separation of electron-hole pairs. The possible mechanism for the enhanced photocatalytic properties of $Ag_3PO_4/Fe_3O_4/GO$ composites is also discussed. With the help of external magnetic field, the photocatalysts can be easily separated from the solution for recycling.

Keywords: Graphene; Silver phosphate; Magnetite; Composites; Photocatalysis.

1. Introduction

In the past decades, many effects have been made to purify contaminated water, which has a severe threat to human beings. Photocatalytic degradation is considered to be the most common and effective method for treating organic pollutants. In recent years, silver orthophosphate (Ag_3PO_4) has become a hot and popular photocatalyst due to its high photooxidative capabilities for oxidation of water and the photodecomposition of organic pollutants under visible-light irradiation [1-3]. However, Ag_3PO_4 is subject to stability issues in practical applications because it can be photoreduced and decomposed to weakly active Ag if no sacrificial reagent is involved [4-6]. Many works have been made to improve the stability while simultaneously further enhance the photocatalytic performance of Ag_3PO_4. Recent report indicated that using insoluble AgX (X = Cl, Br, I) modified Ag_3PO_4 could improve its photocatalytic activity and stability [7]. In addition, combination of Ag_3PO_4 with different supports including TiO_2 [8], SnO_2 [9] and carbon quantum dots [10] has recently been developed to improve the photocatalytic activity and stability of Ag_3PO_4.

Graphene has attracted great attention due to its unique properties, such as large specific surface area, exceptional electrical conductivity, excellent mobility of charge carriers and high chemical stability [11]. Graphene oxide (GO) is the oxidative form of graphene with copious hydroxyl and carboxyl groups on the basal planes and edges, which favor its solubility in solvents and provide opportunities for synthesis of GO-based composites [12-14]. The fabrication of GO-based composites as

photocatalysts, such as ZnO/GO, TiO_2/GO, Ag/AgX/GO (X = Br, Cl) and Ag_2O/GO [15-22] have been reported and they show significantly enhanced photocatalytic performance in the degradation of pollutants due to the efficient charge transportation and separation capacity of GO. Considering the superior properties of GO, the combination of GO and Ag_3PO_4 could also improve the photocatalytic activity of Ag_3PO_4. Up to now, several groups have reported the synthesis of GO-based Ag_3PO_4 photocatalysts with enhanced photocatalytic activity [23-25]. However, it is very difficult to reuse the photocatalysts from the reaction media. Traditional separation is usually expensive and time-consuming. Thereby, it is very important and desirable to develop an effective and facile method to construct photocatalysts which can be easily re-collected from the reaction solution.

Fe_3O_4 nanoparticles have attracted much attention because of their excellent magnetic properties. So far, many methods have been developed to combine Fe_3O_4 nanoparticles with a catalyst to fabricate a new magnetically recyclable catalyst. For example, Ye et al. have successfully synthesized magnetic core/shell structured WO_3/Fe_3O_4 photocatalyst with enhanced photocatalytic activity and stable recyclability [26]. Xuan et al. have developed hollow spherical Fe_3O_4/TiO_2 hybrid photocatalysts with good photocatalytic activity under UV light irradiation and can be recycled by magnetic separation [27]. Zhou et al. have prepared Fe_3O_4/C_3N_4 nanospheres with good porous structure via a hydrothermal method [28]. Mao et al. have reported on the synthesis of magnetically separable Ag_3PO_4/Fe_3O_4 composites [29]. However, to the best of our knowledge, there is no report on the synthesis of

Ag_3PO_4/Fe_3O_4/GO ternary composite photocatalysts.

The aim of the present research is to develop an efficient magnetically recoverable Ag_3PO_4/Fe_3O_4/GO composite photocatalyst. It was found that the presence of GO can improve the photocatalytic activity for the degradation of RhB under simulated sunlight irradiation as compared with pure Ag_3PO_4. Moreover, the photocatalytic performance can be further adjusted by simply changing the content of GO in the Ag_3PO_4/Fe_3O_4/GO composites. The possible mechanism for the enhanced photocatalytic activity was proposed.

2. Experimental

2.1. Materials

Natural flake graphite (99.9% purity) was obtained from Qingdao Guyu Graphite Co., Ltd., with a particle size of 150 μm. All the other chemical reagents involved in this research were analytical grade, purchased from Sinopharm Chemical Reagent Co., Ltd., and used as received without further purification. Deionized (DI) water was used throughout this work.

2.2. Synthesis of the Ag_3PO_4/Fe_3O_4/GO composites

Graphite oxide was synthesized from natural flake graphite by using a modified Hummer method [30,31]. The colloidal suspension of Fe_3O_4 nanocrystals was synthesized by the reported method [32]. In a typical synthesis of the Ag_3PO_4/Fe_3O_4/GO composites, 40 mg of graphite oxide was dispersed in a solution of DI water (40 mL) and ethanol (40 mL) by sonication for about 1 h. Subsequently, 2

mL of the Fe_3O_4 colloidal suspension was added into the above solution. After stirring for about 4 h, 5 mL of $AgNO_3$ (2.5 mmol) aqueous solution was added and stirred for 1 h. Then 10 mL of Na_2HPO_4 (1.0 mmol) aqueous solution was added and stirred for another 1 h. The products were separated by centrifugation, washed with water and ethanol, and then dried in a vacuum oven at 45 °C. For comparison, a series of Ag_3PO_4/Fe_3O_4/GO composites were fabricated by changing the amount of GO and denoted as Ag_3PO_4/Fe_3O_4/GO-*x*, with *x* representing the used amount of GO. Pure Ag_3PO_4 was also obtained through a similar procedure in the absence of GO and Fe_3O_4.

2.3. Characterization of photocatalysts

The crystalline phases of Ag_3PO_4/Fe_3O_4/GO composites were analyzed by X-ray diffraction (XRD) on a Bruker D8 Advance diffractometer with Cu *K*α radiation (λ = 1.5406 Å). The morphology of the obtained samples was determined by field emission scanning electron microscopy (FESEM, JSM-7001F) and transmission electron microscopy (TEM, JEOL JEM-2100). The compositions of the as-prepared products were evaluated by inductively coupled plasma-optical emission spectrometer (ICP-OES, Vista-MPX, Varian). Ultraviolet-visible (UV-vis) spectroscopy measurements were performed on a UV-1800PC UV-vis spectrophotometer. Magnetic property of the sample was evaluated on a HH-15 vibrating sample magnetometer (VSM) at room temperature.

2.4. Photocatalytic activity

The photocatalytic activity of the samples was evaluated by degradation of RhB

dye under simulated sunlight irradiation. A 500 W tungsten lamp as the light source was positioned at *ca*. 10 cm away from the reaction cell to trigger the photocatalytic reaction. In a typical photocatalytic experiment, 30 mg of photocatalyst powder was dispersed in 100 mL of RhB aqueous solution (5 mg L^{-1}) in a Pyrex reactor. Prior to irradiation, the suspension was magnetically stirred for 1 h in the dark to reach the adsorption-desorption equilibrium on the surface of the photocatalyst. Under simulated sunlight irradiation, about 3 mL of the suspension was collected at 5 min intervals and separated through centrifugation. The concentration of RhB was analyzed by measuring the absorbance with a UV-vis spectrophotometer. The characteristic absorption peak was chosen to be 554 nm. The degradation efficiency was calculated using the relative concentration (C/C_0) of RhB as a function of time, where C_0 is the concentration of RhB at adsorption equilibrium, and C is the residual concentration.

3. Results and discussion

3.1. Characterization of as-prepared samples

The strategy for synthesis of the Ag_3PO_4/Fe_3O_4/GO composites is shown in Fig. 1. Due to the plenty of oxygen-containing functional groups (hydroxyl, epoxide and carboxylic groups) on the basal planes of GO nanosheets, GO sheets are highly negatively charged when dispersed in water, Thus the positively charged Fe_3O_4 and Ag^+ ions can absorb on the surface of negatively charged GO sheets. When Na_2HPO_4 was added into the solution, the strong chemical combination occurred between Ag^+

ions and PO_4^{3-} ions, leading to the formation of Ag_3PO_4 particles on GO sheets eventually.

XRD patterns of the as-synthesized graphite oxide, pure Ag_3PO_4, and Ag_3PO_4/Fe_3O_4/GO-40 composites are shown in Fig. 2. In the case of graphite oxide, the obvious diffraction peak located at around 11° corresponds to the (001) diffraction of graphite oxide [33]. For the pattern of pure Ag_3PO_4, all of the diffraction peaks can be indexed to the body-centered cubic structure of Ag_3PO_4 (JCPDS card no. 06-0505). The Ag_3PO_4/Fe_3O_4/GO-40 composites exhibit a similar XRD pattern to that of pure Ag_3PO_4. No obvious diffraction peaks of graphite oxide or Fe_3O_4 are observed in the Ag_3PO_4/Fe_3O_4/GO-40 composites, which is consistent with other reports about GO-based composites [16,34]. The reason could be ascribed to the exfoliation of layer-stacking graphite oxide and the relatively low diffraction intensity of Fe_3O_4 compared to Ag_3PO_4 [32].

The morphological characteristics of the as-prepared pure Ag_3PO_4 and Ag_3PO_4/Fe_3O_4/GO-40 composite were investigated by FESEM, which is shown in Fig. 3. Pure Ag_3PO_4 in the absence of GO sheets is irregular particles with diameters in the range of 0.5-1 μm (Fig. 3a). The Ag_3PO_4 particles and GO sheets (GO sheets were tagged with red arrows) in the Ag_3PO_4/Fe_3O_4/GO-40 composites can be clearly seen in Fig. 3b. The morphology of the Ag_3PO_4 particles in Ag_3PO_4/Fe_3O_4/GO-40 composite is similar to that of the pure Ag_3PO_4, but the size becomes smaller (about 100-250 nm). The smaller size of the Ag_3PO_4 in the hybrid may be due to the existence of GO, which can act as a surfactant in the reaction system and effectively

retard particle aggregations [20,35].

A deeper insight into the detailed structures of the Ag_3PO_4/Fe_3O_4/GO-40 composites is obtained from TEM observations. The crumpled and sheet-like structure is clearly observed for GO sheets, as shown in Fig. 3c. And the GO sheets are decorated randomly with the Ag_3PO_4 particles. Except Ag_3PO_4 particles, there are many much smaller particles anchored on the GO sheets. Fig. 3d is the enlarged TEM image of the area marked by a rectangle in Fig. 3c. The average size of the small particles is 5 nm, which is consistent with the size reported for the Fe_3O_4 nanoparticles [32]. From the high resolution TEM image in the inset of Fig. 3d, the lattice fringes with interplanar distance of approximately 0.252 nm can be indexed to the (311) crystal planes of cubic Fe_3O_4. This result proves the presence of Fe_3O_4 nanoparticles in the Ag_3PO_4/Fe_3O_4/GO composites.

3.2. Magnetic properties

The magnetic property of Ag_3PO_4/Fe_3O_4/GO-40 composite was investigated by VSM at room temperature. Fig. 4 displays the hysteresis loop of Ag_3PO_4/Fe_3O_4/GO-40 composite. Ag_3PO_4/Fe_3O_4/GO-40 composite exhibits a superparamagnetic behavior without observable coercivity and remanence. The saturation magnetization (M_s) of Ag_3PO_4/Fe_3O_4/GO-40 is about 1.56 emu g^{-1}. The smaller M_s value is due to the low content of the magnetite fraction in the composite (2.7%). The magnetic property of the Ag_3PO_4/Fe_3O_4/GO composites facilitates their separation and recycling from the liquid-phase reaction system. As presented in the inset of Fig. 4, upon applying an external magnetic field, the sample could be well

separated from aqueous dispersion by a magnet within 15 seconds. This clearly demonstrates the facile separability of the Ag_3PO_4/Fe_3O_4/GO composites from the reaction media.

3.3. Photocatalytic properties

The photocatalytic performance of the samples was evaluated by photocatalytic degradation of RhB under simulated sunlight irradiation. Temporal concentration changes of RhB were monitored by examining the variations in maximal absorption in UV-vis spectra at 554 nm. For comparison, the catalytic properties of pure Ag_3PO_4 and Ag_3PO_4/Fe_3O_4/GO composites with different GO contents were also investigated. Fig. 5 displays the degradation ratio versus reaction time in the presence of different photocatalysts. When introducing a small amount of GO, the activity of Ag_3PO_4/Fe_3O_4/GO-20 composite is enhanced. This result indicates that GO plays an important role in decomposing the organic pollutant of RhB under simulated sunlight irradiation. In addition, the content of GO in the composites has a great effect on the photocatalytic activities of Ag_3PO_4. With increasing the feeding amount of GO to 40 mg, the degradation ratio of RhB was further increased to 97% within 25 min irradiation. The enhanced photocatalytic activity of Ag_3PO_4/Fe_3O_4/GO composites can be ascribed to the ability of GO to promote the separation of photogenerated carriers, which is also reported by other GO-based composite photocatalysts [15-22]. However, further increasing the GO content leads to the decrease of photocatalytic activity, which could be ascribed to the covering of the active sites on the surface of Ag_3PO_4 [36]. This result indicates that a suitable amount of GO is crucial for

optimizing the photocatalytic activity of $Ag_3PO_4/Fe_3O_4/GO$ composites. In this study, the photocatalytic reactions followed the pseudo-first-order kinetics, as displayed in Fig. 6. The apparent rate constants (k, min^{-1}) are determined from the slopes of $\ln(C/C_0)$ versus irradiation time. The rate constants for Ag_3PO_4 and $Ag_3PO_4/Fe_3O_4/GO$ composites follow the order $Ag_3PO_4/Fe_3O_4/GO$-40 > $Ag_3PO_4/Fe_3O_4/GO$-20 > Ag_3PO_4 > $Ag_3PO_4/Fe_3O_4/GO$-60. The $Ag_3PO_4/Fe_3O_4/GO$ composites synthesized with 40 mg of GO exhibits the best photocatalytic activity. The degradation rate constant for $Ag_3PO_4/Fe_3O_4/GO$-40 composite is 0.138 min^{-1}, which is 2.6 times of pure Ag_3PO_4 (0.054 min^{-1}). Thus, the $Ag_3PO_4/Fe_3O_4/GO$-40 composites were selected for the following experiments.

To investigate the stability of $Ag_3PO_4/Fe_3O_4/GO$-40 composites, the reusability was further evaluated in terms of cycling degradation experiments for three times. All the processes and parameters were kept unchanged during the cycling tests. As shown in Fig. 7, although some loss of photocatalytic activity was observed, the $Ag_3PO_4/Fe_3O_4/GO$-40 composite maintains a relatively high photocatalytic activity during the recycle reaction for photodegradation of RhB. Since the dosage of the photocatalysts is very small, the decrease of the activity during the recycling reactions could be attributed to the loss of some of the catalysts during the photocatalytic processes. It is known that by absorbing incident light, Ag_3PO_4 could be photoreduced to form metallic Ag, which could be evidenced by the XRD pattern of Ag_3PO_4 after three cycling runs (Fig. 8). However, when $Ag_3PO_4/Fe_3O_4/GO$-40 composite was used as the photocatalyst to repeat three cycling runs, there were only small diffraction

peaks of metallic Ag appeared in the XRD pattern, which suggests that GO can inhibit the further production of Ag from the decomposition of Ag_3PO_4 [8].

Generally, photoinduced reactive species including holes, hydroxyl radicals (·OH), and superoxide radicals ($O_2^{\bullet-}$) are expected to be involved in the photocatalytic process. *p*-benzoquinone (BZQ), disodium ethylenediaminetetraacetate (Na_2-EDTA) and isopropanol (IPA) are commonly used as scavenger of $O_2^{\bullet-}$ radicals, holes and ·OH radicals, respectively. To investigate the role of these reactive species, controlled degradation experiments with the addition of BZQ, Na_2-EDTA and IPA were performed. Fig. 9 shows the influences of radical scavengers on the RhB degradation process. The experimental results show that in the presence of IPA, the degradation ratio of RhB has no obvious changes. The addition of BZQ reduces the degradation ratio of RhB to 17%. While in the presence of Na_2-EDTA, the degradation rate of RhB was severely decreased to about 2%. These results suggest that the degradation of RhB with Ag_3PO_4/Fe_3O_4/GO composites as the photocatalyst is mainly attributed to direct oxidation by holes and $O_2^{\bullet-}$ radicals, while ·OH radicals play a comparatively minor role in the degradation process.

Based on the above discussion, a possible mechanism for the photodegradation of RhB over Ag_3PO_4/Fe_3O_4/GO composites is proposed, as shown in Fig. 10. Under simulated sunlight irradiation, electrons (e^-) in the valence band (VB) of Ag_3PO_4 can be excited to its conduction band (CB), causing the generation of holes (h^+) in the VB of Ag_3PO_4 simultaneously. Due to the presence of GO sheets, the photogenerated electrons on the surface of Ag_3PO_4 can transfer to the surface of GO sheets, and thus

promote the separation of photoinduced electron-hole pairs and enhance the photocatalytic activity. The efficient electron transfer from Ag_3PO_4 to GO sheets also can avoid Ag_3PO_4 from photocorrosion, which can inhibit the light absorption and decrease photocatalytic activity. The photogenerated electrons on GO can adsorb surface O_2 to form $O_2^{\bullet-}$ radicals. These $O_2^{\bullet-}$ radicals can efficiently decompose RhB. Meanwhile, the resultant holes (h^+) in the VB of Ag_3PO_4 can oxidize RhB directly because of their strong oxidation. In a word, the effective separation of electrons and holes contributes to the improved photocatalytic performance of Ag_3PO_4/Fe_3O_4/GO composites.

4. Conclusions

In summary, Ag_3PO_4/Fe_3O_4/GO ternary composites with different GO contents are successfully synthesized by an electrostatic interaction combined with a chemical precipitation approach. The Ag_3PO_4/Fe_3O_4/GO composites show much enhanced photocatalytic activity for degradation of RhB. The enhanced photocatalytic activity may be mainly attributed to the existence of GO, which can accelerate the charge separation and inhibit the further decomposition of Ag_3PO_4 into Ag. It is revealed that the direct oxidization of RhB by holes and $O_2^{\bullet-}$ radicals take a major role in the whole degradation process. More importantly, Ag_3PO_4/Fe_3O_4/GO composites can be easily separated from the reaction system by applying an external magnetic field. Thus, the the Ag_3PO_4/Fe_3O_4/GO ternary composites with excellent magnetic and enhanced catalytic properties are expected to a promising material for the environmental issues.

Acknowledgements

The authors are grateful for financial support from National Nature Science Foundation of China (No. 51272094) and the Startup Fund for Distinguished Scholars of Jiangsu University (No. 15JDG023).

Figure Captions

Fig. 1. Synthetic procedure for the $Ag_3PO_4/Fe_3O_4/GO$ composites.

Fig. 2. XRD patterns of (a) graphite oxide, (b) pure Ag_3PO_4, and (c) $Ag_3PO_4/Fe_3O_4/GO$-40 composite.

Fig. 3. FESEM images of (a) pure Ag_3PO_4 and (b) $Ag_3PO_4/Fe_3O_4/GO$-40 composites. (c) TEM image of the $Ag_3PO_4/Fe_3O_4/GO$-40 composite and (d) the enlarged TEM image of the area marked by a rectangle in (c).

Fig. 4. Field-dependent magnetization curve of $Ag_3PO_4/Fe_3O_4/GO$-40 composite at room temperature (the inset shows the magnetic separation of the catalyst).

Fig. 5. Time profiles of RhB degradation over different catalysts under simulated sunlight irradiation.

Fig. 6. The pseudo-first-order plots of ln(C/C_0) *vs* reaction time in the presence of different photocatalysts.

Fig. 7. Repeated photocatalytic degradation of RhB with $Ag_3PO_4/Fe_3O_4/GO$-40 as photocatalysts.

Fig. 8. XRD patterns of pure Ag_3PO_4 and $Ag_3PO_4/Fe_3O_4/GO$-40 photocatalysts after three cycle experiments.

Fig. 9. Photocatalytic activity of $Ag_3PO_4/Fe_3O_4/GO$-40 for RhB with different scavenges under simulated sunlight irradiation.

Fig. 10. Proposed photocatalytic mechanism for the degradation of RhB over $Ag_3PO_4/Fe_3O_4/GO$ composites under simulated sunlight irradiation.

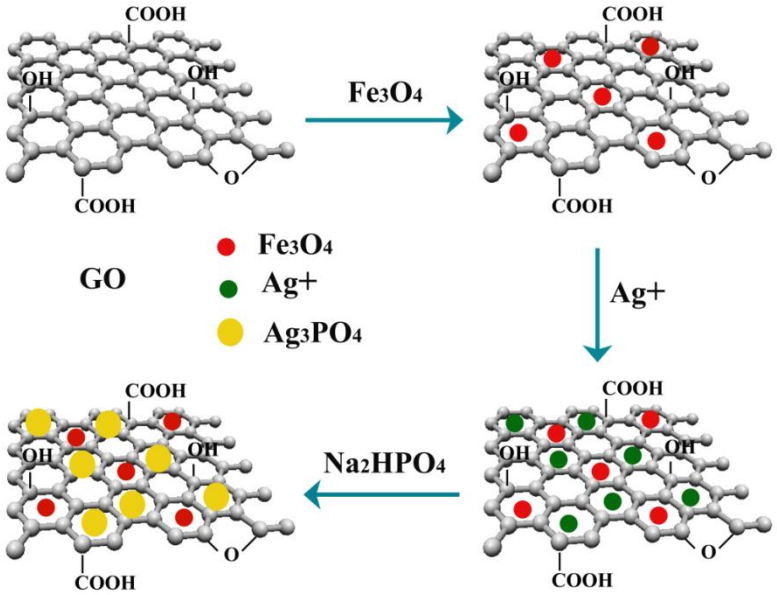

Figure 1

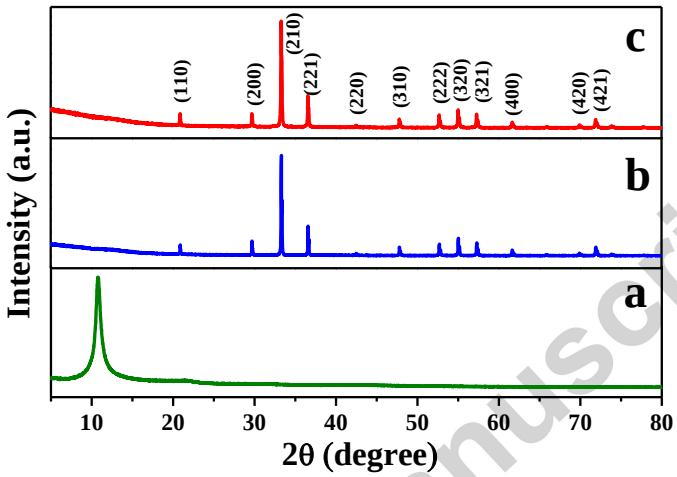

Figure 2

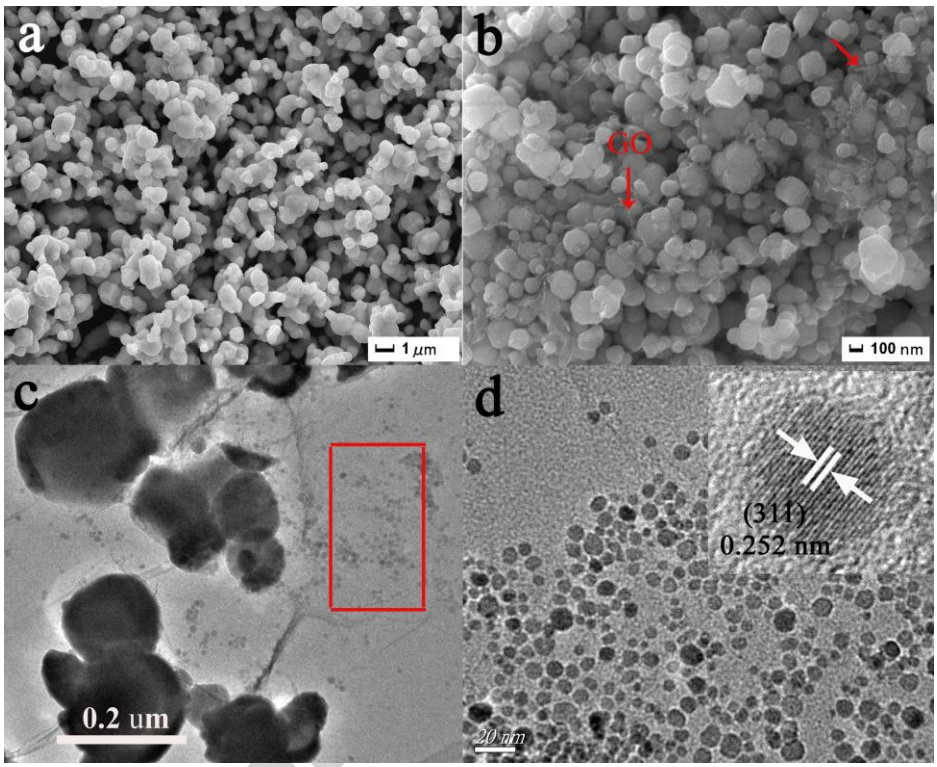

Figure 3

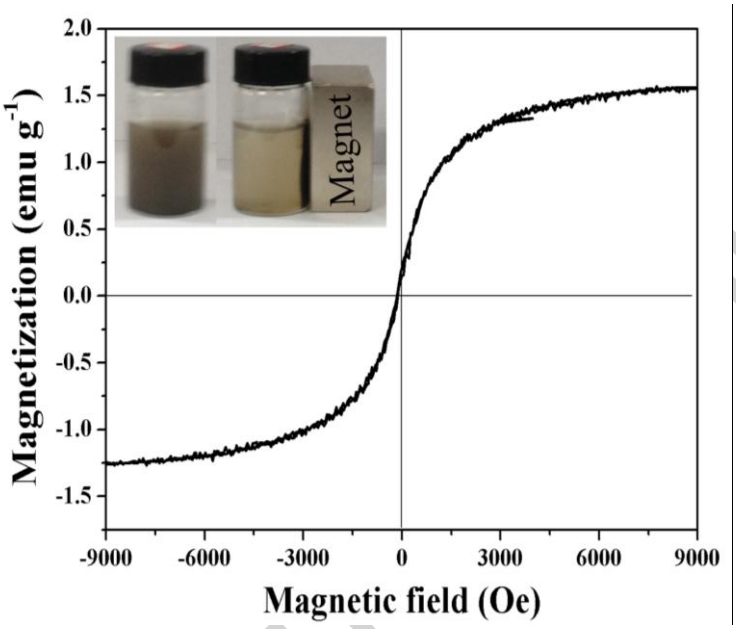

Figure 4

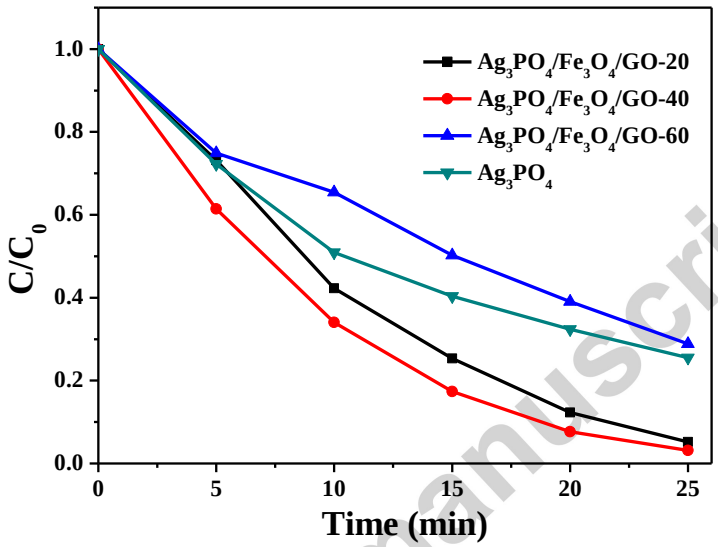

Figure 5

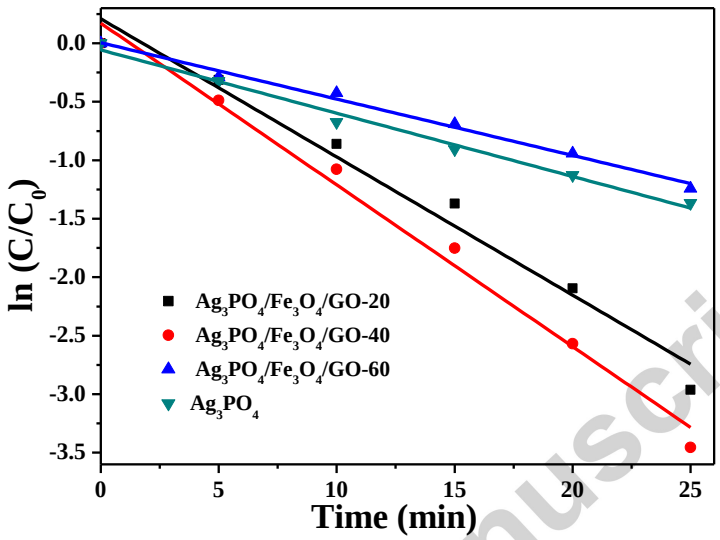

Figure 6

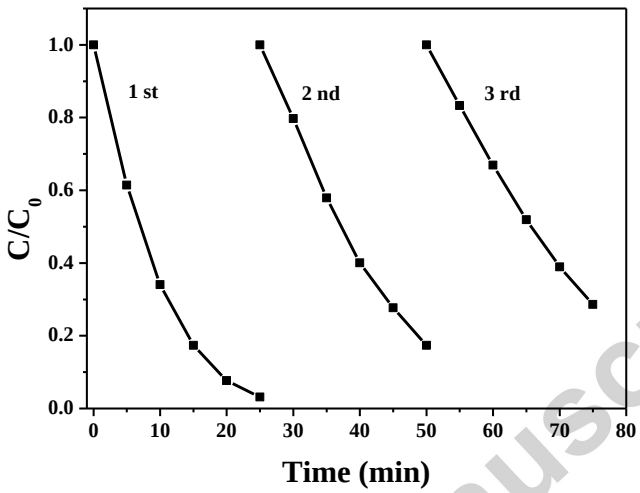

Figure 7

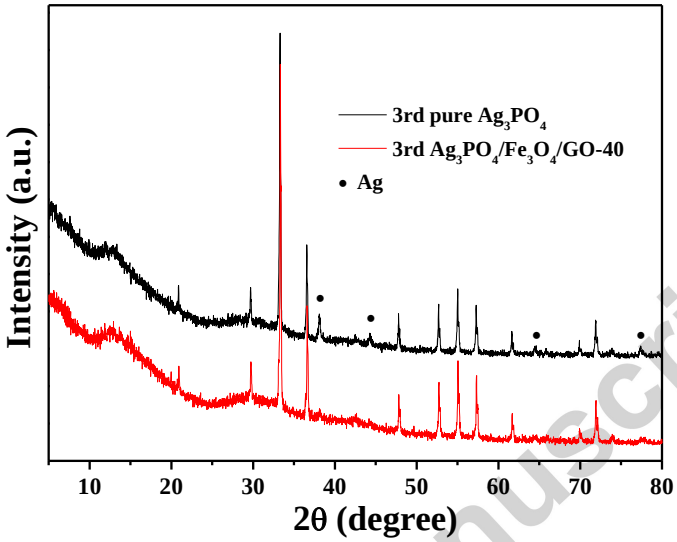

Figure 8

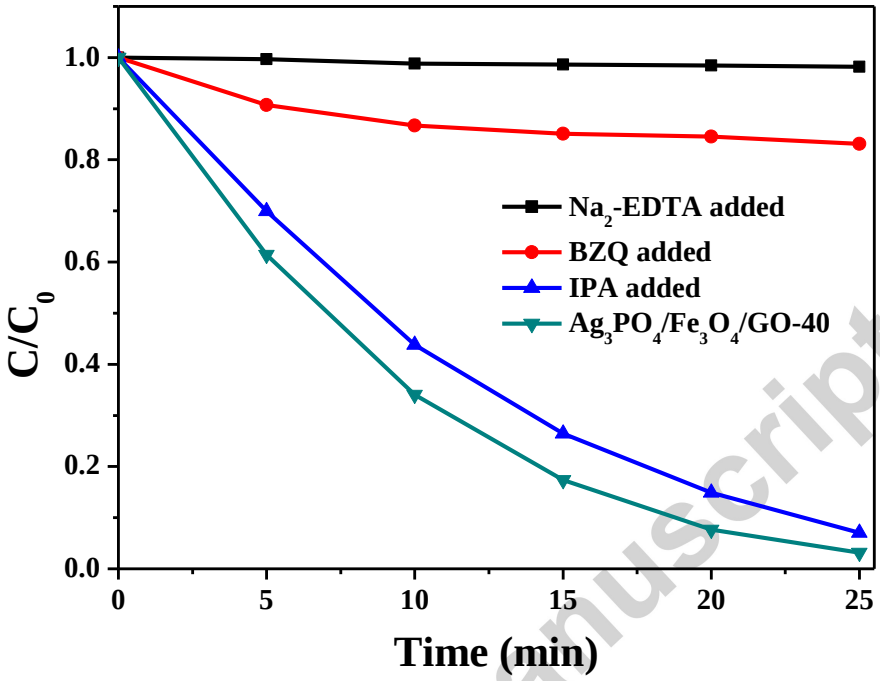

Figure 9

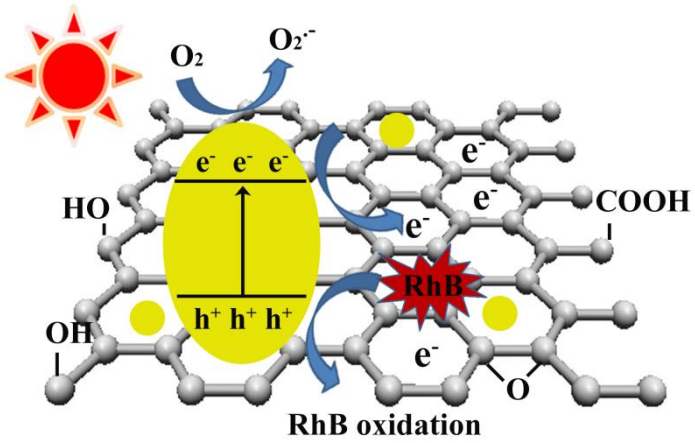

Figure 10

References

[1] Z.G. Yi, J.H. Ye, N. Kikugawa, T. Kako, S.X. Ouyang, H. Stuart-Williams, H. Yang, J.Y. Cao, W.J. Luo, Z.S. Li, Y. Liu, An orthophosphate semiconductor with photooxidation properties under visible-light irradiation, Nat. Mater. 9 (2010) 559-564.

[2] Y.P. Bi, S.X. Ouyang, N. Umezawa, J.Y. Cao, J.H. Ye, Facet effect of single-crystalline Ag_3PO_4 sub-microcrystals on photocatalytic properties, J. Am. Chem. Soc. 133 (2011) 6490-6492.

[3] Y.P. Bi, H.Y. Hu, S. Ouyang, G.H. Lu, J.Y. Cao, J.H. Ye, Photocatalytic and photoelectric properties of cubic Ag_3PO_4 sub-microcrystals with sharp corners and edges, Chem. Commun. 48 (2012) 3748-3750.

[4] H. Wang, Y.S. Bai, J.T Yang, X.F Lang, J.H Li, L. Guo, A facile way to rejuvenate Ag_3PO_4 as a recyclable highly efficient photocatalyst, Chem. Eur. J. 18 (2012) 5524-5529.

[5] M. Ge, N. Zhu, Y.P. Zhao, J. Li, L. Liu, Sunlight-assisted degradation of dye pollutants in Ag_3PO_4 suspension, Ind. Eng. Chem. Res. 51 (2012) 5167-5173.

[6] Y.P. Liu, L. Fang, H.D. Lu, L.J Liu, H. Wang, C.Z. Hu, Highly efficient and stable Ag/Ag_3PO_4 plasmonic photocatalyst in visible light, Catal.Commun. 17 (2012) 200-204.

[7] Y.P. Bi, S. Ouyang, J.Y. Cao, J.H. Ye, Facile synthesis of rhombic dodecahedral AgX/Ag_3PO_4 (X=Cl, Br, I) heterocrystals with enhanced photocatalytic properties and stabilities, Phys. Chem. Chem. Phys. 13 (2011) 10071-10075.

[8] W.F. Yao, B. Zhang, C.P. Huang, C. Ma, X.L. Song, Q.J. Xu, Synthesis and characterization of high efficiency and stable Ag_3PO_4/TiO_2 visible light photocatalyst for the degradation of methylene blue and rhodamine B solutions, J. Mater. Chem. 22 (2012) 4050-4055.

[9] L.L. Zhang, H.C. Zhang, H. Huang, Y. Liu, Z.H. Kang, Ag_3PO_4/SnO_2 semiconductor nanocomposites with enhanced photocatalytic activity and stability, New J.Chem. 36 (2012) 1541-1544.

[10] H.C. Zhang, H. Huang, H. Ming, H.T. Li, L.L. Zhang, Y. Liu, Z.H. Kang, Carbon quantum dots/Ag_3PO_4 complex photocatalysts with enhanced photocatalytic activity and stability under visible light, J. Mater. Chem. 22 (2012) 10501-10506.

[11] V. Singh, D. Joung, L. Zhai, S. Das, S.I. Khondaker, S. Seal, Graphene based materials: Past, present and future, Prog. Mater. Sci. 56 (2011) 1178-1271.

[12] D.W. Boukhvalov, M.I. Katsnelson, Modeling of graphite oxide, J. Am. Chem. Soc. 130 (2008) 10697-10701.

[13] D.R. Dreyer, S. Park, C.W. Bielawski, R.S. Ruoff, The chemistry of graphene oxide, Chem. Soc. Rev. 39 (2010) 228-240.

[14] N.R. Wilson, P.A. Pandey, R. Beanland, R.J. Young, I.A. Kinloch, L. Gong, Z. Liu, K. Suenaga, J.P. Rourke, S.J. York, J. Sloan, Graphene oxide: Structural analysis and application as a highly transparent support for electron microscopy, ACS Nano 3 (2009) 2547-2556.

[15] H. Zhang, X.J. Lv, Y.M. Li, Y. Wang, J.H. Li, P25-graphene composite as a high performance photocatalyst, ACS Nano 4 (2010) 380-386.

[16] J.C. Liu, H.W. Bai, Y.J. Wang, Z.Y. Liu, X.W. Zhang, D.D. Sun, Self-assembling TiO_2 nanorods on large graphene oxide sheets at a two-phase interface and their anti-recombination in photocatalytic applications, Adv. Funct. Mater. 20 (2010) 4175-4181.

[17] C. Chen, W.M. Cai, M.C. Long, B.X. Zhou, Y.H. Wu, D.Y. Wu, Y.J. Feng, Synthesis of visible-light responsive graphene oxide/TiO_2 composites with p/n heterojunction, ACS Nano 4 (2010) 6425-6432.

[18] J.C. Liu, L. Liu, H.W. Bai, Y.J. Wang, D.D. Sun, Gram-scale production of graphene oxide–TiO_2 nanorod composites: Towards high-activity photocatalytic materials, Appl. Catal., B 106 (2011) 76-82.

[19] T.G. Xu, L.W. Zhang, H.Y. Cheng, Y.F. Zhu, Significantly enhanced photocatalytic performance of ZnO via graphene hybridization and the mechanism study, Appl. Catal., B 101 (2011) 382-387.

[20] M.S. Zhu, P.L. Chen, M.H. Liu, Graphene oxide enwrapped Ag/AgX (X=Br, Cl) nanocomposite as a highly efficient visible-light plasmonic photocatalyst, ACS Nano 5 (2011) 4529-4536.

[21] H. Zhang, X.F. Fan, X. Quan, S. Chen, H.T. Yu, Graphene sheets grafted Ag@AgCl hybrid with enhanced plasmonic photocatalytic activity under visible light, Environ. Sci. Technol. 45 (2011) 5731-5736.

[22] Z.Y. Ji, X.P. Shen, J.L. Yang, Y.L. Xu, G.X. Zhu, K.M. Chen, Graphene oxide modified Ag_2O nanocomposites with enhanced photocatalytic activity under visible-light irradiation, Eur. J. Inorg. Chem. 36 (2013) 6119-6125.

[23] G.D. Chen, M. Sun, Q. Wei, Y.F. Zhang, B.C. Zhu, B. Du, Ag_3PO_4/Graphene-oxide composite with remarkably enhanced visible-light-driven photocatalytic activity toward dyes in water, J. Hazard. Mater. 244-245 (2013) 86-93.

[24] Q.H. Liang, Y. Shi, W.J. Ma, Z. Li, X.M. Yang, Enhanced photocatalytic activity and structural stability by hybridizing Ag_3PO_4 nanospheres with graphene oxide sheets, Phys. Chem. Chem. Phys. 14 (2012) 15657-15665.

[25] L. Liu, J.C. Liu, D.D. Sun, Graphene oxide enwrapped Ag_3PO_4 composite: towards a highly efficient and stable visible-light-induced photocatalyst for water purification, Catal. Sci. Technol. 2 (2012) 2525-2532.

[26] G. Xi, B. Yue, J.Y. Cao, J.H. Ye, Fe_3O_4/WO_3 Hierarchical core-shell structure: high-performance and recyclable visible-light photocatalysis, Chem. Eur. J. 17 (2011) 5145-5154.

[27] S.H. Xuan, W.Q. Jiang, X.L. Gong, Y. Hu, Z.Y. Chen, Magnetically separable Fe_3O_4/TiO_2 hollow spheres: fabrication and photocatalytic activity, J. Phys. Chem. C 113 (2009) 553-558.

[28] X.S. Zhou, B. Jin, R.Q. Chen, F. Peng, Y.P. Fang, Synthesis of porous Fe_3O_4/g-C_3N_4 nanospheres as highly efficient and recyclable photocatalysts, Mater. Res. Bull. 48 (2013) 1447-1452.

[29] G.P. Li, L.Q. Mao, Magnetically separable Fe_3O_4-Ag_3PO_4 sub-micrometre composite: facile synthesis, high visible light-driven photocatalytic efficiency, and good recyclability, RSC Adv. 2 (2012) 5108-5111.

[30] W.S. Hummers, R.E. Offeman, Preparation of graphitic oxide, J. Am. Chem. Soc. 80 (1958) 1339-1339.

[31] Z.Y. Ji, X.P. Shen, J.L. Yang, G.X. Zhu, K.M. Chen, A novel reduced graphene oxide/Ag/CeO_2 ternary nanocomposite: Green synthesis and catalytic properties, Appl. Catal. B 144 (2014) 454-461.

[32] G.X. Zhu, Y.J. Liu, Z. Xu, T. Jiang, C. Zhang, X. Li, G. Qi, Flexible magnetic nanoparticles-reduced graphene oxide composite membranes formed by self-assembly in solution, ChemPhysChem 11 (2010) 2432-2437.

[33] T. Nakajima, A. Mabuchi, R. Hagiwara, A new structure model of graphite oxide, Carbon 26 (1988) 357-361.

[34] L. Liu, J.C. Liu, D.L. Sun, Graphene oxide enwrapped Ag_3PO_4 composite: towards a highly efficient and stable visible-light-induced photocatalyst for water purification, Catal. Sci. Technol. 2 (2012) 2525-2532.

[35] R. Pasricha, S. Gupta, A.K. Srivastava, A facile and novel synthesis of Ag-graphene-based nanocomposites, Small, 5 (2009) 2253-2259.

[36] J. Zhang, J.G. Yu, M. Jaroniec, J.R. Guo, Noble metal-free reduced graphene oxide-$Zn_xCd_{1-x}S$ nanocomposite with enhanced solar photocatalytic H_2-production performance, Nano Lett. 12 (2012) 4584-4589.